Heliyon 9 (2023) e16971

Contents lists available at ScienceDirect

Heliyon

journal homepage: www.cell.com/heliyon

Magnetic graphene oxide, a suitable support in ficin immobilization

Z. Tahsiri [a], M. Niakousari [a,*], A. Niakowsari [b]

[a] Department of Food Science and Technology, College of Agriculture, Shiraz University, Shiraz, Iran
[b] Departments of Communication and Electronics, School of Computer and Electrical Engineering, Shiraz University, Shiraz, Iran

ARTICLE INFO

Keywords:
Enzyme immobilization
Ficin
Graphene oxide
Graphite

ABSTRACT

In the present study, we aimed to develop a fast, non-toxic ultrasonic-assisted technique for the preparation of graphene oxide (GO) and GO that were accessorized with Fe_3O_4 (GO-Fe_3O_4) for enzyme immobilization. The structural properties of nanosheets were determined by FTIR, XRD, and SEM. Immobilized enzymes on the GO-Fe_3O_4 and GO were counted. Enzyme activity, reusability, and improvements in enzyme stability were studied. According to the results, the immobilization efficiency was 256.86 mg ficin/GO (g), and 253.63 mg ficin/GO-Fe_3O_4 (g). Furthermore, immobilized ficin was affected in terms of stability by variations in pH and temperature. The immobilized ficin on the GO-Fe_3O_4 could be easily recycled from the reaction medium by applying external magnetic separation, involving 10 cycles for 120 days. Over this period and with this number of cycles, the immobilized enzyme on the GO-Fe_3O_4 retained 74% of its original activity, whereas the immobilized enzyme on the GO was recycled from the reaction medium after centrifuging, thereby retaining 70% of its original activity. Thus, GO and GO-Fe_3O_4 nanosheets were obtained efficiently from the ultrasonic-assisted technique and can be regarded as excellent nanocarriers for enzyme immobilization.

1. Introduction

Enzymes are often recognized as smart and native biocatalysts. Their immobilization is highly valued in manufacturing numerous industrial products such as biofuels, pharmaceuticals, drugs, food, and chemicals [1]. Due to substantial differences in the material properties of each carrier and enzyme-loading capacity, the best carrier type is yet to be finalized for efficient enzyme immobilization [2]. An enzyme carrier can be based on graphene oxide (GO) and be applied successfully in several biologically-active apparatuses, such as biosensors, novel biocatalysts, and drug delivery vehicles [3,4]. As the enzyme is adsorbed onto GO, it provides high enzyme loading capacity, low diffusional resistance, and a large surface area [5]. A previous case of research revealed that GO is characterized by multiple advantages, e.g. high pore volume, biodegradability, and thermal stability, which make it an appropriate option for enzyme/biomolecule immobilization [6]. Furthermore, different oxygenated functional groups, including carboxyl, epoxy, and hydroxyl groups on the surface of GO can facilitate bonding between GO and inorganic nanoparticles, thereby allowing the formation of different GO-based hybrids [7,8]. Meanwhile, there have been two main strategies for the specific purpose of GO preparation. These methods are, namely, mechanical exfoliation and chemical oxidation-reduction [9]. There are limits on the mass-scale production of GO through mechanical exfoliation, usually because of low yields and high costs. However, the Hummers' method, which relies on

* Corresponding author.
E-mail addresses: mehrnia2012@yahoo.com, niakosar@shirazu.ac.ir (M. Niakousari).

https://doi.org/10.1016/j.heliyon.2023.e16971
Received 13 November 2022; Received in revised form 23 May 2023; Accepted 2 June 2023
Available online 2 June 2023

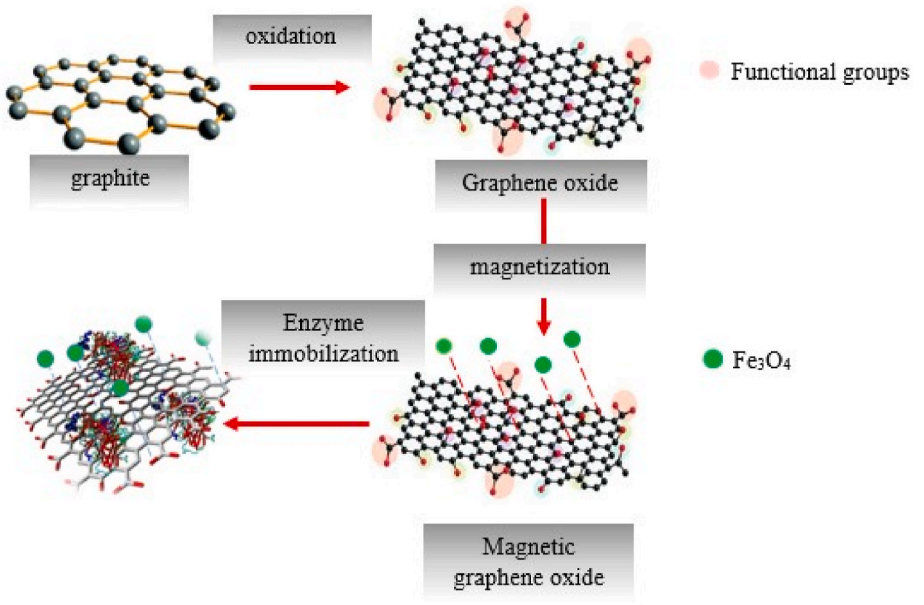

Fig. 1. Schematic showing the ficin immobilization on the GO–Fe_3O_4 nanosheets.

oxidation-reduction, has the disadvantage of generating pollutants but remains a common method. Several other drawbacks of this method include the release of byproducts, such as heavy metal ions, and a high risk of explosion due to the presence of unstable Mn_2O_7 intermediates [9,10]. Moreover, GO usually shows poor solubility when produced by conventional methods [11]. Thus, it is obvious that another method is needed to produce graphene oxide. GO production is preferably assisted by ultrasonic methods, as an efficient, fast, and probably environmentally-friendly technique for GO production. Meanwhile, it makes large inter-layer spaces and few-layer counts that neither produce toxic gases nor have the disadvantages of the Hummers' method [12]. Furthermore, oxygenated groups which are generated on the surface of GO via the oxidation of carbon atoms during the ultrasonic process could be connected to various molecules that can make it a good option for enzyme immobilization and magnetic nanoparticle binding. The use of a magnetic nanocarrier is preferable to a non-magnetic nanocarrier for enzyme immobilization because of its ability to recover immobilized enzymes by applying an external magnetic field to the reaction medium. Thus, sonication can be a desirable method to prepare magnetic graphene oxide. As GO binds with Fe_3O_4, magnetic nanosheets are made as a site for enzyme immobilization and for recycling the enzymes from the reaction medium [13]. To the best of our knowledge, numerous studies have considered relevant aspects in this field, such as the removal of Azo dye from wastewater by immobilized lipase on the GO [14], enzyme cocktail immobilization on magnetic graphene oxide for the enhancement of operational stability of sugarcane bagasse hydrolyzing [15], use of immobilized cellulases and xylanases on the magnetic graphene oxide for the production of cellulosic ethanol [16], and the immobilization of glucoamylase and xylanase enzymes on functional magnetic graphene oxide. These indicated that using hydrophilic crosslinkers such as cyanuric chloride and polyethylene glycol bis amin assisted in improving the catalytic properties of the enzymes by changing the microenvironment of the mentioned immobilized enzyme [17]. Graphene oxide was produced by the conventional method in all of the cases mentioned above. However, there is a knowledge gap in the current understanding of enzyme immobilization on GO and Fe_3O_4–bound GO (i.e. GO-Fe_3O_4) produced by ultrasonic-assisted methods. To date, there has been no research on their usage as convenient and unique nanosheets for protease immobilization. As one of the first enzymes applied by humans in food processing, protease is commonly used [18,19] because of its various applications in biotechnology, ranging from the synthesis of amino acids to the production of bioactive peptides from inexpensive proteins, ultimately for enhancing functional and organoleptic properties of foods [20–22]. While being a chemical alternative, protease avoids the destruction of some amino acids and the occurrence of by-products [23]. Consumers reportedly showed less interest in using proteases from mammalian sources [24] due to the risk of disease transmission, whereas recombinant proteases cannot be applied in human foods in some countries [25]. Among the most prevalent types of applicable proteases with plant-based origin, ficin has particular importance [26]. It has been used in pharmaceuticals, brewing, and the production of bioactive peptides. Ficin has also been recognized for its ability to generate a reproducible hydrolysis map and is known to have applications in the production of antibodies through specific hydrolysis [27]. In this study, we modified the conventional Hummer's method ($KMnO_4$, H_2SO_4/H_3PO_3) by an ultrasound-assisted approach to decrease the temperature and reaction time of graphite oxidation. We made a large amount of GO and GO-Fe_3O_4 with more hydrophilic groups which resulted from a high level of oxidation due to acoustic cavitation, leading to locally high pressures and temperatures. Furthermore, in this method, we did not need to use $NaNO_3$ for oxidation so that toxic NO_2/N_2O_4 gas would not be generated. Accordingly, we developed a nontoxic, ultrafast, ultrasound-assisted procedure to use high-quality GO and GO-Fe_3O_4 as platforms for the immobilization of ficin (EC 3.4.22.3) for the first time. To assess the efficiency of our work, FTIR, XRD, and SEM were applied on the said

nanosheets. The enzyme immobilization process is described in Fig. 1. Ultimately, several features of the free ficin were compared with those of the immobilized ficin in the GO and GO-Fe_3O_4 nanosheets. In a comparative approach, these features were, namely, enzyme-loading capacity, enzyme activity, reusability, stability against pH change, and thermal stability.

2. Materials and methods

2.1. Materials

Caseinate sodium and ficin (EC 3.4.22.3, from fig tree latex, as powder, ≥0.1 unit/mg solid) were purchased from Sigma Aldrich Co. USA. Other chemicals included Coomassie brilliant blue G250, di-sodium hydrogen phosphate (Na_2HPO_4), sodium dihydrogen phosphate (NaH_2PO_4), sodium hydroxide (NaOH), graphite powder (300 mush), hydrogen peroxide (H_2O_2), sulfuric acid 98% (H_2SO_4), potassium ferrate (K_2FeO_4), potassium hydroxide (KOH), hydrazine hydrate (H_6N_2O), potassium permanganate ($KMnO_4$), sodium nitrate ($NaNO_3$), phosphorus acid (H_3PO_3). All were of analytical grade and were purchased from Merck Chemical Co. Germany.

2.2. Synthesis of GO and magnetic GO

GO was synthesized according to Liu's method with some changes [28]. For this purpose, 6 g of K_2FeO_4 was added to 400 mL of H_2SO_4 (98%) at room temperature. Then, 1 g of graphite powder was dispersed into the said mixture which, in turn, was exposed to the ultrasound in a bath for 1 h. At this stage, the GO and Fe^{+2}/Fe^{+3} solutions were created and then separated into 2 portions. In the first portion, Fe^{+2}/Fe^{+3} and graphene oxide were separated in a solution using dialysis, a semi-permeable membrane that allows the penetration of Fe^{+2}/Fe^{+3}. The remaining colloidal solution in the dialysis bag, which contains graphene oxide but not iron ions, was then centrifuged. The centrifuged sediments, i.e. graphene oxide, were then separated and collected for further evaluations. The second portion was adjusted to a pH value of 12 by adding KOH (1 M) dropwise into the solution. This was followed by the addition of 1 mL hydrazine monohydrate. The suspension was exposed to ultrasound in a bath for 45 min at 30 °C and, subsequently, the mixture was dialyzed for 72 h against distilled water to eliminate any reagents and remaining materials. Finally, the GO-Fe_3O_4 was obtained through centrifugation. The GO-Fe_3O_4 were synthesized by co-precipitation of $FeCl_3{\cdot}6H_2O$ and $FeCl_2{\cdot}4H_2O$ in the presence of GO prepared through Hummer's method [29,33]. However, this was time-consuming in comparison with Liu's modified method. Therefore, the magnetic GO in the present study was prepared by the latter.

2.3. Dynamic light scattering (DLS)

The zeta potential and particle size of GO and GO-Fe_3O_4 nanosheets were determined through the DLS technique using a Zetasizer (ZS-100, Horiba, Japon) at 25 °C based on dynamic light scattering methods. According to a protocol by Hegedűs et al. [30], the samples were tested in stoppered glass bottles and, prior to the measurements, they were homogenized by ultrasonic waves for 5 min. The zetasizer used a 633 nm HeNe laser in backscatter mode at an angle of 173°.

2.4. Ficin immobilization

To allow conjugation between ficin and GO nanosheets, first, a dispersion (2.5 mg/mL) of GO and GO-Fe_3O_4 was prepared. Accordingly, each GO nanosheet was sampled (10 mg) and dispersed in 4 mL of sodium phosphate buffer (10 mM, pH 7). Each dispersion was mixed thoroughly with 0.1 mL ficin (5 mg/mL) and 4.8 mL distilled water for 2–12 h at ambient temperature. The immobilized ficin was isolated from nanosheets at hour-to-hour intervals by applying an external magnetic field or through centrifugation. The Bradford method was used for evaluating the extent of immobilization of ficin on various nanosheets by measuring the initial (Ci) and final (Cs) concentrations of protein in the reaction medium at 595 nm by the colorimetric method, thereby enabling speed and precision. The amino acid composition of the measured proteins is known to affect the outcome of the reaction. Immobilization efficiency (%) was calculated according to Eq. (1):

$$Immobilization\ efficiency\ (\%) = (ci - cs\ /\ ci) \times 100 \quad (1)$$

2.5. X-ray diffraction (XRD)

An assessment of X-ray diffraction was applied on a Bruker D8-advance in the range of 10–80° with monochromatic CuKα1 radiation (0.15406 nm). The LECO CHNS-932 analyzer was used for elemental analysis [10].

2.6. Fourier transformed-infrared (FTIR) spectra

The GO hybrids were compacted with KBr into a pellet. The infrared absorption spectra were obtained via Nicolet Nexus 470 Fourier transform spectrometer (Thermo Fisher Scientific, Waltham, U.K.). The spectra ranged from 400 to 4000 cm^{-1} at a resolution of 4 cm^{-1} [28].

Table 1
Particle size and Zeta potential of nanosheets.

Sample	Average hydrodynamic diameter (nm)	Zeta-potential
GO	125.00 ± 16.59	−42.00 ± 0.00
GO-Fe_3O_4	195.00 ± 11.83	−37.00 ± 0.00

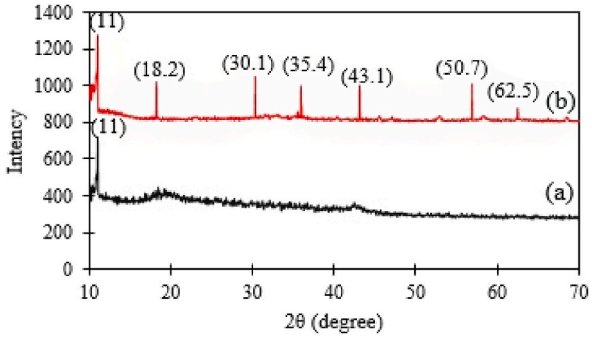

Fig. 2. XRD pattern of GO (a) and GO-Fe_3O_4 (b).

2.7. Analysis of microstructure by scanning electron microscopy (SEM)

The microstructures of GO hybrids were determined by scanning electron microscopy. Sample preparation was done by pouring 20 μL of the dispersion on Sellotape which was placed on the sample holder. Then, the liquid content evaporated and the remaining materials on the sample holder were sputtered with gold. All the images were obtained on a Vega3, TESCAN, Brno, Czech microscope at an accelerating voltage of 20 kV.

2.8. Enzyme activity measurement

The enzyme unit, abbreviated as 1 U, is a measure of an enzyme's catalytic activity and is defined as the quantity of the enzyme required to catalyze the conversion of 1 μmol of substrate per minute, under specific conditions required by the assay's protocol. The proteolytic activity of ficin was estimated by the Kunitz and Devaraj method [31]. The stock solution of casein (1% w/v) was made by dissolving 1 g casein in 99 mL sodium phosphate buffer (10 mM, pH 7) that contained 5 mM cysteine hydrochloride. To enable measurements of proteolytic activity, 1 mL of the enzyme (1% W/V) was added to 1 mL of casein solution. The mixture remained on a shaker for 20 min and was left to stand at 60 °C. The reactions were terminated after 10-min by adding 2 mL of trichloroacetic acid (10%). Immobilized ficin was collected by an external magnetic field and the absorbance of the remaining solution was measurable at 280 nm.

2.9. Determination of temperature and pH stability of the immobilized ficin

To determine the temperature-related stability of free and immobilized enzyme activity, the enzyme was first incubated in a sodium phosphate buffer (50 mM, pH 7) and was then exposed to 40, 50, 60, 70, and 80 °C as separate batches. Then, the enzymatic activities of each incubated batch of immobilized enzyme were measured at 37 °C according to Kunitz and Devaraj.

The samples were preincubated on various buffer solutions, with pH values that ranged from 4 to 9 at 60 °C. The pre-incubation determined the optimum pH value of the enzyme. Various buffers were used for achieving different ranges of pH values. They included the Tris–HCl buffer (50 mM, pH 8–9), potassium phosphate buffer (50 mM, pH 6–7), and citrate buffer (50 mM, pH 4–6). After pre-incubating the different buffers, which had different pH values, the residual enzyme activities were measured at pH 7 and 60 °C.

2.10. The activity and reusability of immobilized ficin

The stability and reusability of immobilized ficin were inspected by assaying ficin activity repeatedly at pH 7 (4 °C) for 120 days, with 20-day intervals. For this purpose, the enzyme was incubated with sodium caseinate as substrate and, after each run, the enzyme was separated from the reaction medium through an external magnetic field. When appropriate, it was rinsed with phosphate buffer (pH 7) several times, thereby removing the remaining substrate and product, so that the residual enzyme activity could be determined. Twenty days later, the next experiment was performed in a condition akin to that of the previous experiment on the immobilized enzyme. Storage conditions were set at pH 7 and 4 °C, lasting for 20 days.

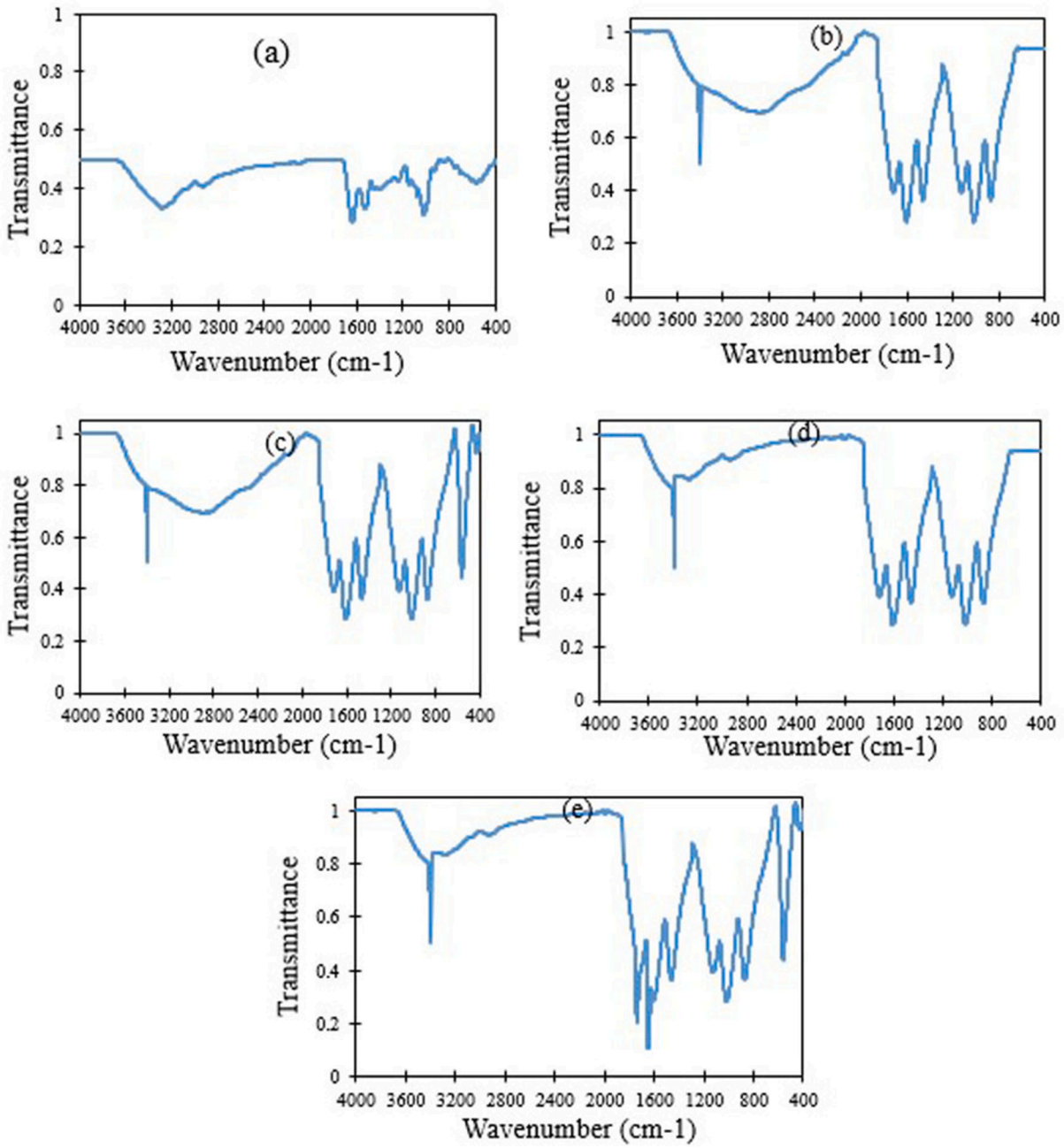

Fig. 3. FTIR spectra of ficin (a), GO (b), GO-Fe_3O_4 (c), ficin immobilized on the GO (d), ficin immobilized on the GO-Fe_3O_4 (e)

2.11. Statistical analysis

All treatments were carried out in triplicates. The analysis of variance (one-way ANOVA) was performed by SPSS 24 (SPSS Inc., Chicago, IL, USA) software. Tukey's test was used for determining significant differences among mean values ($p < 0.05$).

3. Results and discussion

3.1. Characterization of GO nanoparticles

According to the results of dynamic light scattering (Table 1), the average hydrodynamic diameter of GO and GO-Fe_3O_4 showed similar sizes that ranged approximately from 125 to 195 nm. As shown in Table 1, the zeta potential of GO was −42 mV because of

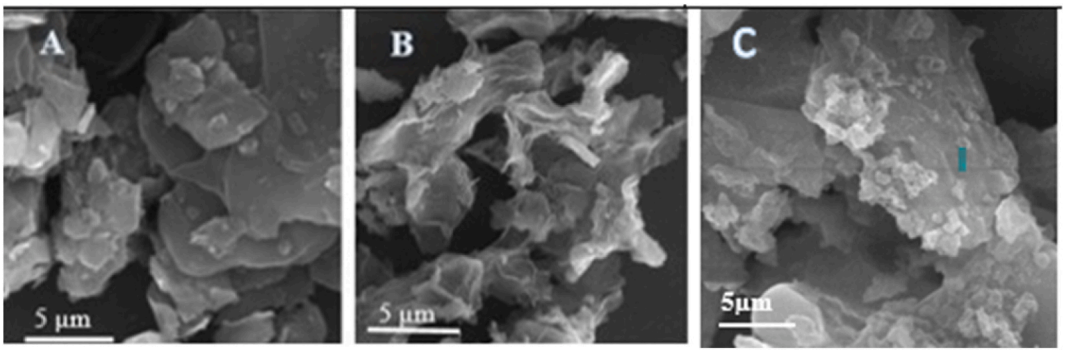

Fig. 4. SEM images of graphite −700× (a), GO-700× (b) and GO-Fe_3O_4-700× (c).

Table 2
mg of immobilized ficin/gr GO-Fe_3O_4 and GO.

Time (h)	GO-Fe_3O_4/ficin	GO/ficin
2	51.60 ± 0.71^{gK}	53.65 ± 0.55^{hK}
3	85.13 ± 1.01^{fJ}	86.90 ± 0.15^{gJ}
4	134.10 ± 1.38^{eI}	138.39 ± 1.27^{fH}
5	171.08 ± 1.07^{dG}	173.67 ± 1.78^{eG}
6	188.97 ± 1.17^{cF}	191.64 ± 1.63^{dFG}
7	250.63 ± 0.38^{aAB}	256.86 ± 0.79^{aA}
8	240.54 ± 1.14^{bDE}	243.27 ± 1.40^{bcC}
9	242.12 ± 0.20^{bC}	245.98 ± 0.68^{bB}
10	240.39 ± 0.74^{bD}	242.08 ± 0.64^{bcC}
11	239.21 ± 0.98^{bD}	241.68 ± 0.48^{bcE}
12	240.68 ± 0.49^{bDE}	241.00 ± 2.44^{cE}

Different lowercase letters within a column and uppercase letters within a row show significant ($p < 0.05$) differences.

–COOH and –OH groups. This value increased to −37 mV in the case of GO-Fe_3O_4 because Fe_3O_4 nanoparticles had a positive charge (29 mV), thereby confirming relevant research in the available literature [32].

By showing the crystal texture of samples, the XRD pattern can reveal success in GO-Fe_3O_4 hybrid fabrication. The x-ray diffraction patterns (XRD) of GO and GO-Fe_3O_4 revealed significant differences (Fig. 2). The diffraction pattern of GO demonstrated that $2\theta = 11$, thereby confirming similar measurements in a previous case of research [33]. The diffraction peak at 42° indicates the presence of natural graphite and its complete oxidation with functional groups which contain oxygen [34]. While the ultrasound treatment causes an asymmetric micro jet to be made on graphite, the collapse of cavitation bubbles usually leads to erosion on the surface of graphite particles, thereby causing interlayer spacing. These few layers and the formation of the expanded structure of graphite can add to the local pressure and increase the temperature due to transient hot spots. Accordingly, suitable sites are produced for oxidation among epoxy and carboxylic groups in between the layers of GO [10,35]. The diffraction peaks of GO-Fe_3O_4 match magnetic Fe_3O_4 structures according to JCPDS files no. 19–629.

The spectrum of ficin, GO and GO-Fe_3O_4 as well as ficin immobilized on the GO-Fe_3O_4 is shown in Fig. 3. The GO and GO-Fe_3O_4 displayed characteristics of the peaks in the C–O carboxyl (V_{C-O} at 1051 cm^{-1}), C–O epoxy (V_{C-O} at 1274 cm^{-1}), C]C ($V_{C]C}$ at 1615 cm^{-1}), adsorbed water molecules (V_{O-H} at 1627 cm^{-1}), C]O ($V_{C]O}$ at 1728 cm^{-1}) and O–H (V_{O-H} at 3000-3600 cm^{-1}). The spectra of GO-Fe_3O_4 showed a new peak at 580 cm^{-1} corresponding to the Fe–O stretch vibration which appeared because the Fe_3O_4 was incorporated into the GO [36]. A clear peak at 3390 cm^{-1} appeared in the GO and GO-Fe_3O_4 spectra, indicating that GO nanosheets had absorbed water. The existence of epoxy and carboxyl groups on the GO nanosheets showed that functional groups containing oxygen, during the oxidation of graphite, entered the carbon skeleton so that the extended cross-linked π-orbital system of the original graphite was destroyed. The existence of C]C also indicated remnants of the sp^2 orbital [37]. The high intensities of the oxygen-containing functional groups such as $V_{C]O}$, V_{C-O}, and V_{O-H}, as well as hydroxyl groups such as V_{C-O-H} showed that graphite was oxidized completely because of the ultrasound treatment. This finally led to hydrophilic moieties of the GO nanosheets. On the one hand, sonication assisted in the emergence of active sites and facilitated the interspersion of carbon layers, including epoxide, carboxyl, and hydroxyl functionality in the reaction. On the other hand, it offered more advantages in alleviating extreme pressure, high temperature, and fast cooling rates as a result of the cavitation. Ultimately, this facilitated the oxidation reaction at lower temperatures and in shorter durations, compared to the conventional Hummer's method [10,38]. The diffraction peaks of the conjugated forms between ficin and GO-Fe_3O_4 indicated a broad spectrum of absorption, regarding amine and its stretching vibration at 3410–3450 cm^{-1}. The C–N stretching vibration appeared at 1392 cm^{-1}. Furthermore, the occurrence of spectral peaks at 1731 cm^{-1} and 1645 cm^{-1} of the asymmetric and symmetric forms of the C]O stretching vibration can be assigned to the carboxylic acid and

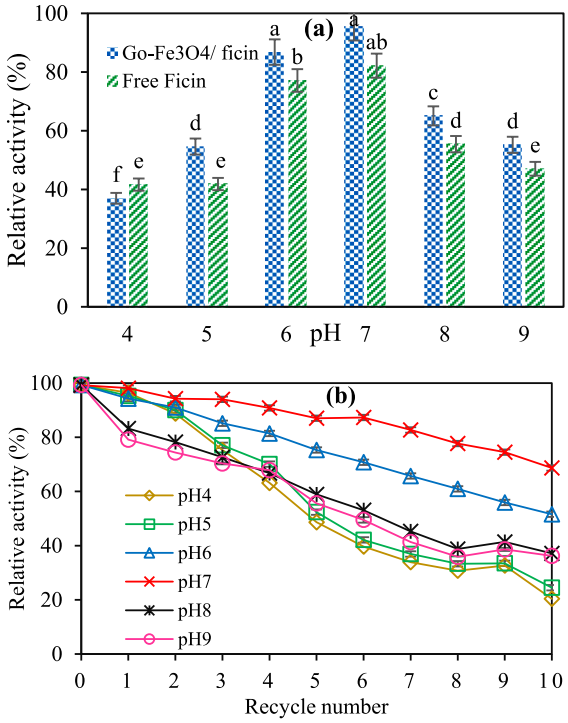

Fig. 5. (a) Effect of pH value on the relative activity of free and immobilized ficin on GO-Fe_3O_4. (b) The reusability of the immobilized ficin on the GO-Fe_3O_4 nanocarrier at different pH values and a constant temperature of 60 °C.

amide groups, respectively.

The morphology of graphite, GO and GO-Fe_3O_4 were examined using scanning electron microscopy. As shown in Fig. 4, sonication effectively exfoliated GO sheets by destroying their structure. This occurrence ultimately expanded the surface area of GO. Furthermore, a comparison of the morphologies revealed that GO consisted of a more porous and wrinkled structure than graphite. This difference possibly resulted from the microjets and shockwave at the solid-liquid interface when GO nanosheets were produced [39]. The SEM image of GO-Fe_3O_4 nanosheets (Fig. 4c) clearly shows nanoparticles with different morphologies, compared to non-magnetic GO that formed on the GO layers. In sum, sonication resulted in a higher surface area and a more narrow-size distribution [35].

3.2. Ficin immobilization and its activity at optimum values of temperature and pH

Ficin immobilization on the GO and GO-Fe_3O_4 occurred through the incubation of ficin and the nanosheets at pH 7 and room temperature. The immobilization efficiency was measured according to a relevant method in the literature (Section 2.4). According to Table 2., the optimum incubation time was 7 h for enzymes immobilized on the GO-Fe_3O_4 and GO. Increasing the time from 2 to 7 h resulted in a steady increase in the amount of incubated ficin (mg) and, thereafter, no significant changes occurred for up to 12 h. Meanwhile, the amounts of enzyme incubation on the graphene oxide and magnetic graphene oxide were not significantly different from each other. The immobilization efficiencies for GO and GO-Fe_3O_4 were 256.86 and 253.63 mg ficin, respectively. Applying sonication during the preparation of GO and GO-Fe_3O_4 not only created a more porous structure, along with a greater surface area, but also allowed the placement of hydrophilic groups such as hydroxyl and carboxyl, thereby preventing the aggregation of the GO nanosheets. For this reason, despite the magnetized nature of graphene oxide, with Fe_3O_4, there was no significant difference in the amount of enzyme immobilized on the GO, compared to its magnetic counterpart. In this study, the magnetization of graphene oxide only enabled an easier separation of the enzyme and did not affect the inhibition of GO aggregation. In fact, GO nanosheets that are produced through ultrasound treatment do not usually aggregate in aqueous solutions since the nanosheets have hydrophilic groups in their structure.

The initial activity of ficin was 0.1 units/mg of enzyme, which was considered the relative activity out of 100%. The optimal pH was 7 and the optimal temperature was 60 °C for free ficin activity. The reusability of immobilized ficin was determined in the said conditions. After each run, the immobilized ficin that had been separated through the external magnetic field was rinsed, and its activity was measured as stated previously. This cycle was repeated for up to 10 times. At first, ficin activities were assayed at temperatures between 40 and 80 °C with intervals of 10 °C and at a constant pH (7). In the pH range of 4–9, however, the activities were assayed at pH values of 4, 5, 6, 7, 8, and 9, at a constant temperature of 60 °C. The activities of immobilized ficin at 60 °C and pH 7 resulted in recovery rates of approximately 92% and 97%, respectively.

The stability of pH value in the case of free and immobilized ficin at 60 °C (Fig. 5a and b) can be seen in association with thermal

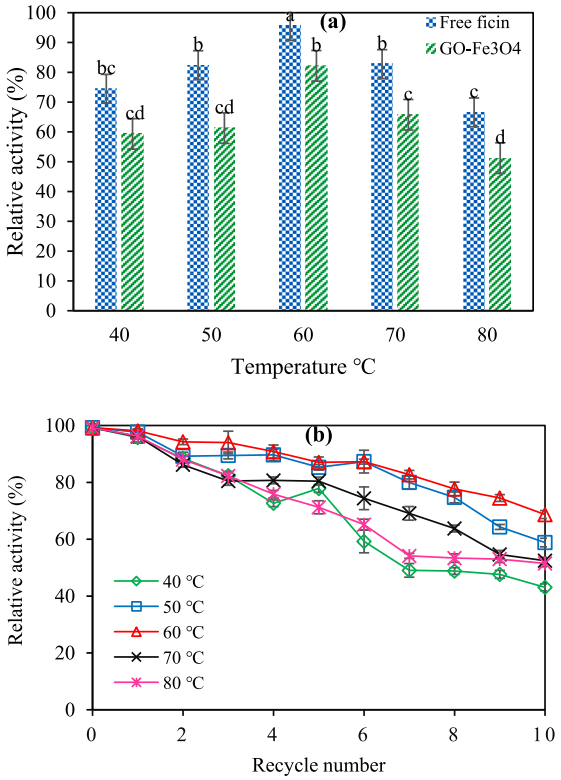

Fig. 6. (a) Effect of temperature on the activity of free and immobilized ficin on GO-Fe_3O_4. (b) The reusability of the immobilized ficin on the GO-Fe_3O_4 nanocarrier at different temperatures and a constant pH value of 7.

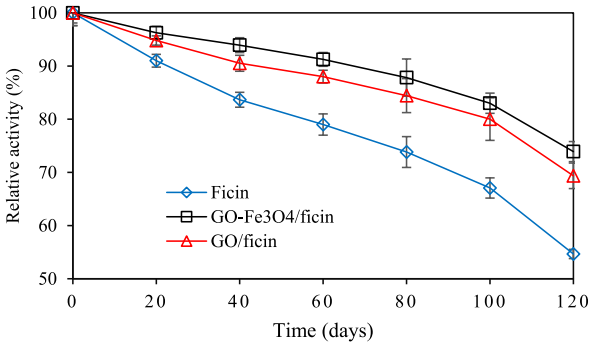

Fig. 7. The long-term storage stability of free and immobilized ficin on GO and GO-Fe_3O_4.

stability at pH 7 (Fig. 6a and b). The results confirmed significant improvements in enzyme stability after immobilization, probably due to the occurrence of more structural rigidity of ficin in response to the immobilization [40,41]. In Figs. 5a and 6a, the results revealed that the stability of ficin changed in response to the pH and temperature. These changes were significantly greater than those observed in free ficin, perhaps because of an expanded porous structure and the features of enzyme/GO-Fe_3O_4 binding, which enhanced the protection of ficin against denaturation [33].

3.3. Storage and reusability of immobilized ficin

The reusability of an enzyme can be considered an important advantage in the provision of economic industrial production. Reusability, long term stability, and enhanced activity may be realized through enzyme immobilization on solid supports such as nanosheets. The storage stability of free and immobilized ficin on the GO and GO-Fe_3O_4 was measurable at 4 °C (pH 7) over a period of 120 days. The immobilized ficin on the GO and GO-Fe_3O_4 lost 30% and 26% of its original activity, respectively. Regarding free ficin, however, the decrease in activity was almost 50% of the initial ficin activity (Fig. 7.). The activity of immobilized ficin was higher than

that of the free enzyme, probably because of the covering effect of nanosheets on the enzyme which may assist in preventing conformational changes. Furthermore, these led to smaller distortion effects that were caused by the aqueous medium. Weaker distortions meant that the active site of ficin became less affected so that the immobilization could occur efficiently [42].

4. Conclusion

The present work showed that the ultrasound treatment shortened the reaction time required for the synthesis of the GO nanocarrier, compared to the reaction time in the Hummer's method. In conclusion, the present research developed a nontoxic, fast, direct, and one-step reaction for the scaleable production of GO and magnetic GO. A simple magnetic separation technique can be used to rapidly separate and recover the magnetic GO bound enzyme from an aqueous solution. This study's findings demonstrate how magnetic separation technology and magnetic composites based on graphene oxide can be used to manage enzyme activity. Multiple characterization methods such as FT-IR spectra, XRD patterns, SEM, and light scattering could be used for demonstrating that GO-Fe_3O_4 hybrids were successfully made. The GO-Fe_3O_4 hybrids had a high level of dispersibility and significant magnetic properties. More importantly, GO-Fe_3O_4 hybrid surfaces were introduced with functional groups that could be used for immobilization. Ficin revealed a strong affinity for absorption onto the surface of magnetic GO because of its large loading capacity. Since the recovery and reusability of enzymes in industrial applications are considered key factors for successful operations, the immobilization of ficin in this study not only enabled the reusability of enzyme through separation by an external magnetic force but also enhanced the enzyme's thermal stability and decreased its susceptibility to changes in pH value. In future research, using hydrophilic cross linkers, such as cyanuric chloride, on the GO may improve the catalytic reaction more effectively. These qualities make this immobilization method an appropriate option for industrial enzyme applications.

Author contribution statement

All authors listed have significantly contributed to the development and the writing of this article.

Data availability statement

Data will be made available on request.

Declaration of competing interest

The authors declare that they have no known competing financial interests or personal relationships that could have appeared to influence the work reported in this paper.

Acknowledgment

The authors would like to express their sincere appreciations to Iran National Science Foundation (INSF) for partially funding this project (Project No. 4002276).

References

[1] A. Basso, S. Serban, Industrial applications of immobilized enzymes—a review, Mol. Catal. 479 (2019), 110607, https://doi.org/10.1016/j.mcat.2019.110607.
[2] S.K. Patel, et al., Eco-friendly composite of Fe3O4-reduced graphene oxide particles for efficient enzyme immobilization, ACS Appl. Mater. Interfaces 9 (3) (2017) 2213–2222, https://doi.org/10.1021/acsami.6b05165.
[3] R. Kumar, P. Pal, Lipase immobilized graphene oxide biocatalyst assisted enzymatic transesterification of Pongamia pinnata (Karanja) oil and downstream enrichment of biodiesel by solar-driven direct contact membrane distillation followed by ultrafiltration, Fuel Process. Technol. 211 (2021), 106577, https://doi.org/10.1016/j.fuproc.2020.106577.
[4] W. Xie, M. Huang, Immobilization of Candida rugosa lipase onto graphene oxide Fe3O4 nanocomposite: characterization and application for biodiesel production, Energy Convers. Manag. 159 (2018) 42–53, https://doi.org/10.1016/j.enconman.2018.01.021.
[5] M. Adeel, et al., Graphene and graphene oxide: functionalization and nano-bio-catalytic system for enzyme immobilization and biotechnological perspective, Int. J. Biol. Macromol. 120 (2018) 1430–1440, https://doi.org/10.1016/j.ijbiomac.2018.09.144.
[6] R.A. Sheldon, D. Brady, Broadening the scope of biocatalysis in sustainable organic synthesis, ChemSusChem 12 (13) (2019) 2859–2881, https://doi.org/10.1002/cssc.201900351.
[7] H. Huang, et al., Facile fabrication of carboxyl groups modified fluorescent C60 through a one-step thiol-ene click reaction and their potential applications for biological imaging and intracellular drug delivery, J. Taiwan Inst. Chem. Eng. 86 (2018) 192–198, https://doi.org/10.1016/j.jtice.2018.02.004.
[8] B. Yu, et al., Adsorption behaviors of tetracycline on magnetic graphene oxide sponge, Mater. Chem. Phys. 198 (2017) 283–290, https://doi.org/10.1016/j.matchemphys.2017.05.042.
[9] M. Cardinali, et al., Radiofrequency plasma assisted exfoliation and reduction of large-area graphene oxide platelets produced by a mechanical transfer process, Chem. Phys. Lett. 508 (4–6) (2011) 285–288, https://doi.org/10.1016/j.cplett.2011.04.065.
[10] T. Soltani, B.-K. Lee, Low intensity-ultrasonic irradiation for highly efficient, eco-friendly and fast synthesis of graphene oxide, Ultrason. Sonochem. 38 (2017) 693–703, https://doi.org/10.1016/j.ultsonch.2016.08.010.
[11] X. Sun, et al., Nano-graphene oxide for cellular imaging and drug delivery, Nano Res. 1 (3) (2008) 203–212. https://link.springer.com/article/10.1007/s12274-008-8021-8.
[12] M. Li, et al., Fingerprinting photoluminescence of functional groups in graphene oxide, J. Mater. Chem. 22 (44) (2012) 23374–23379. https://pubs.rsc.org/en/content/articlelanding/2012/jm/c2jm35417a/unauth.
[13] J.K. Grewal, M. Kaur, Effect of core-shell reversal on the structural, magnetic and adsorptive properties of Fe2O3-GO nanocomposites, Ceram. Int. 43 (18) (2017) 16611–16621, https://doi.org/10.1016/j.ceramint.2017.09.051.

[14] L.W. Yao, et al., Insight into immobilization efficiency of Lipase enzyme as a biocatalyst on the graphene oxide for adsorption of Azo dyes from industrial wastewater effluent, J. Mol. Liq. 354 (2022), 118849, https://doi.org/10.1016/j.molliq.2022.118849.
[15] F.R. Paz-Cedeno, et al., Stability of the Cellic CTec2 enzymatic preparation immobilized onto magnetic graphene oxide: assessment of hydrolysis of pretreated sugarcane bagasse, Ind. Crop. Prod. 183 (2022), 114972, https://doi.org/10.1016/j.indcrop.2022.114972.
[16] F.R. Paz-Cedeno, et al., Magnetic graphene oxide as a platform for the immobilization of cellulases and xylanases: ultrastructural characterization and assessment of lignocellulosic biomass hydrolysis, Renew. Energy 164 (2021) 491–501, https://doi.org/10.1016/j.renene.2020.09.059.
[17] A. Soozanipour, A. Taheri-Kafrani, Enzyme immobilization on functionalized graphene oxide nanosheets: efficient and robust biocatalysts, in: Methods in Enzymology, Elsevier, 2018, pp. 371–403, https://doi.org/10.1016/bs.mie.2018.06.010.
[18] P. Fernandes, Enzymes in food and feed industries: where tradition meets innovation, in: Biocatalysis, Springer, 2019, pp. 233–253. https://link.springer.com/chapter/10.1007/978-3-030-25023-2_12.
[19] A. Vogel, O. May, Industrial Enzyme Applications, John Wiley & Sons, 2019, https://doi.org/10.1002/9783527813780.ch1_1.
[20] O.L. Tavano, Protein hydrolysis using proteases: an important tool for food biotechnology, J. Mol. Catal. B Enzym. 90 (2013) 1–11, https://doi.org/10.1016/j.molcatb.2013.01.011.
[21] M. Esmaeilpour, et al., Antimicrobial activity of peptides derived from enzymatic hydrolysis of goat milk caseins, Comp. Clin. Pathol. 25 (3) (2016) 599–605. https://link.springer.com/article/10.1007/s00580-016-2237-x.
[22] G. Di Pierro, et al., Antioxidant activity of bovine casein hydrolysates produced by Ficus carica L.-derived proteinase, Food Chem. 156 (2014) 305–311, https://doi.org/10.1016/j.foodchem.2014.01.080.
[23] A. Masuda, N. Dohmae, Automated protein hydrolysis delivering sample to a solid acid catalyst for amino acid analysis, Anal. Chem. 82 (21) (2010) 8939–8945, https://doi.org/10.1021/ac101718x.
[24] B. Schnettler, et al., Acceptance of a food of animal origin obtained through genetic modification and cloning in South America: a comparative study among university students and working adults, Food Sci. Technol. 35 (2015) 570–577. https://www.scielo.br/j/cta/a/MV6tBGLGkgL3XffSdkPXHWM/abstract/?lang=en.
[25] R. Morellon-Sterling, et al., Ficin: a protease extract with relevance in biotechnology and biocatalysis, Int. J. Biol. Macromol. 162 (2020) 394–404, https://doi.org/10.1016/j.ijbiomac.2020.06.144.
[26] E.-H. Siar, et al., Immobilization/stabilization of ficin extract on glutaraldehyde-activated agarose beads. Variables that control the final stability and activity in protein hydrolyses, Catalysts 8 (4) (2018) 149, https://doi.org/10.3390/catal8040149.
[27] V. Sączyńska, et al., Production of highly and broad-range specific monoclonal antibodies against hemagglutinin of H5-subtype avian influenza viruses and their differentiation by mass spectrometry, Virol. J. 15 (1) (2018) 1–13. https://virologyj.biomedcentral.com/articles/10.1186/s12985-017-0886-2.
[28] Y. Liu, et al., A facile strategy for preparation of magnetic graphene oxide composites and their potential for environmental adsorption, Ceram. Int. 44 (15) (2018) 18571–18577, https://doi.org/10.1016/j.ceramint.2018.07.081.
[29] W.S. Hummers Jr., R.E. Offeman, Preparation of graphitic oxide, J. Am. Chem. Soc. 80 (6) (1958), https://doi.org/10.1021/ja01539a017, 1339–1339.
[30] T.m. Hegedűs, et al., Specific ion effects on aggregation and charging properties of Boron nitride nanospheres, Langmuir (2021), https://doi.org/10.1021/acs.langmuir.0c03533.
[31] M. Kunitz, Crystalline soybean trypsin inhibitor II. General properties, J. Gen. Physiol. 30 (4) (1947) 291–310, https://doi.org/10.1085/jgp.30.4.291.
[32] Y.-S. Huang, Y.-J. Lu, J.-P. Chen, Magnetic graphene oxide as a carrier for targeted delivery of chemotherapy drugs in cancer therapy, J. Magn. Magn. Mater. 427 (2017) 34–40, https://doi.org/10.1016/j.jmmm.2016.10.042.
[33] M. Royvaran, et al., Functionalized superparamagnetic graphene oxide nanosheet in enzyme engineering: a highly dispersive, stable and robust biocatalyst, Chem. Eng. J. 288 (2016) 414–422, https://doi.org/10.1016/j.cej.2015.12.034.
[34] M. Han, et al., Effect of surface modification of graphene oxide on photochemical stability of poly (vinyl alcohol)/graphene oxide composites, J. Ind. Eng. Chem. 18 (2) (2012) 752–756, https://doi.org/10.1016/j.jiec.2011.11.122.
[35] Z. Zhang, et al., Enhancement of crystallization processes by power ultrasound: current state-of-the-art and research advances, Compr. Rev. Food Sci. Food Saf. 14 (4) (2015) 303–316, https://doi.org/10.1111/1541-4337.12132.
[36] K. Yang, et al., Re-examination of characteristic FTIR spectrum of secondary layer in bilayer oleic acid-coated Fe3O4 nanoparticles, Appl. Surf. Sci. 256 (10) (2010) 3093–3097, https://doi.org/10.1016/j.apsusc.2009.11.079.
[37] Y. Dong, et al., Graphene oxide–iron complex: synthesis, characterization and visible-light-driven photocatalysis, J. Mater. Chem. 1 (3) (2013) 644–650. https://pubs.rsc.org/en/content/articlelanding/2013/ta/c2ta00371f/unauth.
[38] E.C. Vreeland, D.L. Huber, 6 Synthesis and Biomedical Applications of Magnetic Particles, 2020, p. 123.
[39] J. Shen, et al., Synthesis of hydrophilic and organophilic chemically modified graphene oxide sheets, J. Colloid Interface Sci. 352 (2) (2010) 366–370, https://doi.org/10.1016/j.jcis.2010.08.036.
[40] X. Li, et al., One-pot polylol synthesis of graphene decorated with size-and density-tunable Fe3O4 nanoparticles for porcine pancreatic lipase immobilization, Carbon 60 (2013) 488–497, https://doi.org/10.1016/j.carbon.2013.04.068.
[41] F. Gao, et al., Enhancing the catalytic performance of chloroperoxidase by co-immobilization with glucose oxidase on magnetic graphene oxide, Biochem. Eng. J. 143 (2019) 101–109, https://doi.org/10.1016/j.bej.2018.12.013.
[42] T. Nematian, et al., Lipase immobilized on functionalized superparamagnetic few-layer graphene oxide as an efficient nanobiocatalyst for biodiesel production from Chlorella vulgaris bio-oil, Biotechnol. Biofuels 13 (1) (2020) 1–15. https://link.springer.com/article/10.1186/s13068-020-01688-x.